Fast Analysis of Vessel Encoded ASL Perfusion and Angiographic Images

M. A. Chappell[1,2], T. W. Okell[2], S. J. Payne[1], P. Jezzard[2], and M. W. Woolrich[2]
[1]Institute of Biomedical Engineering, University of Oxford, Oxford, United Kingdom, [2]FMRIB Centre, University of Oxford, Oxford, United Kingdom

Introduction: Vessel Encoded Arterial Spin Labelled (VEASL) preparations have been used to provide vessel selectivity in both perfusion and angiographic imaging [1-3]. By spatially modulating the ASL label over a number of cycles, blood in individual arteries is uniquely labelled and its contribution can be extracted during post-processing. Recently a general framework for the analysis of VEASL images has been proposed [4]. This permits the contributions of each feeding artery to be extracted even when the number of unique encoding cycles is limited and where there is some ambiguity in the locations of the arteries in the labelling plane, for example if there has been patient motion after the planning acquisition has been performed. However, a limitation of the framework, as proposed, was the long computation times associated with the analysis, making in infeasible in clinical applications where robust analysis is most critical. Here we propose faster optimization approaches to arrive at the solution, which makes the framework practical for wider application, especially for high-resolution dynamic angiographic datasets.

Methods: Analysis of VEASL data requires voxelwise determination of the contribution from each labelled artery. This can be done with an encoding matrix that specifies the label contribution of each artery for each imaging cycle [1,2], the voxelwise flow contributions being calculated by inversion of this matrix and multiplication with the measured signal vector. However, this solution is sensitive to the accuracy with which the labelling geometry is known and the number of cycles of data acquired. The general framework (GF) for VEASL analysis [4] overcame these limitations by inferring the entries in the encoding matrix from the data (via the locations of the arteries in the labelling plane), and by introducing classification, whereby voxels were assumed only to be fed by a subset of the arteries. The resulting analysis had two stages 1) estimation of 'global' parameters: artery locations and classification proportions, 2) voxelwise calculation of flow contributions. The original demonstration of the GF employed a sampling strategy for Step 1 making it time consuming (~hours for typical perfusion data). To achieve a reduction in computational cost whilst retaining accuracy a number of solutions were explored: A) avoidance of Step 1 by taking 'default' values for the global parameters, i.e. artery locations as estimated from a time-of-flight (TOF) image, this is analogous to a conventional encoding matrix inversion analysis, but with classification applied, B) estimation of 'global' parameters using a non-linear optimization method, C) as B, but instead of estimating artery locations individually it was assumed that the locations could be defined from a TOF image that might have been subject to a small rigid body transformation, e.g. due to motion, with the three parameters of this transformation being estimated, D) as C, but also estimating the flow speed within the arteries [4] to account for this effect on the encoding profile.

To provide objective measures of the relative accuracy of the different approaches we simulated VEASL dynamic angiographic data that contained 4 arteries, with the positions in the imaging plane randomly generated. An example can be seen in Fig. 1. Artery locations in the labelling plane were defined such that the arteries sat at the corners of a square, these locations were subject to a 3 DOF transformation whose parameters were sampled at random (normally distributed with standard deviation of 1 mm for translations and 1° for rotations); the locations chosen before transformation were used to initialise the analyses (as if these were derived from the planning acquisition and there had been subsequent patient motion). The speed of flow in each vessel (which affects the labelling profile) was also randomly perturbed about a 30 cm/s mean (standard deviation 5 cm/s). Data were generated for 8 encoding cycles (tag, control, 2 left-right, 2 anterior-posterior and 2 oblique) and white noise with an effective SNR of 1:10 relative to the flow magnitude was added to the final images. 100 datasets were generated and analysed using standard encoding matrix inversion (MI) and the methods outlined above, assuming in the classification that 2 vessels may contribute to the flow in any voxel. The root-mean-squared-error (RMSE) of the estimated vessel flow contributions was calculated for comparison of the methods.

As an example, the proposed analysis approaches were also applied to VEASL dynamic angiographic [3] data from a healthy subject containing 6 encoding cycles (tag, control, 2 LR, 2 AP) and VEASL perfusion data from different healthy subject containing 8 encoding cycles (tag, control, 2 LR, 2 AP, 2 oblique). The 'global' parameter estimation was performed within a mask derived from a threshold on the signal magnitude (to define the major arteries) in the first frame for the angiographic data (7242 voxels in mask from a 256x256 matrix size) and within a brain mask for the perfusion data (57344 voxels from a 64x64x24 matrix size).

Results: Fig. 1 shows an example set of results from the simulated data, MI performs poorly, whereas both GF solutions shown were able to separate all four artery contributions, the largest discrepancy occurring in areas where three arteries coincide. Fig. 2 shows the RMSE across all 100 simulated datasets for all the methods considered. Accuracy was highest in all cases where the vessel locations were inferred from the data with constraints (C and D). GF analysis using the (inaccurate) vessel locations (A) still resulted in an improvement over simple matrix inversion. Table 1 gives the computation time for the dynamic angiographic and perfusion datasets. The colour-coded images of the first frame of the angiographic data are shown in figure 3. MI failed to produce interpretable images on this dataset, the other methods resulted in similar vessel separation, excepting some variation in the left posterior cerebral artery, method D apparently producing the 'cleanest' separation. Colour-coded images for the example perfusion data are given in Fig. 4.

Discussion: These results suggest that the GF can be implemented in a form that is sufficiently fast for routine use with VEASL data in place of encoding matrix inversion or clustering methods. Method A is a natural replacement for encoding matrix inversion, since it similarly uses previously estimated vessel locations and can be computed in a very short time frame, whilst offering greater robustness to ill conditioning. Where vessel locations are not known, for example randomly encoded VEASL [5], or may deviate from the estimated values, a fast optimization procedure can be used that is likely to be comparable in computation time to clustering analysis. The use of optimization to estimate the 'global' parameters in the GF mean that time to compute will vary from subject-to-subject. However, the times given here are typical of those seen for similar resolution VEASL dynamic angiographic images, making robust VEASL analysis possible in clinical applications such as vessel occlusive diseases.

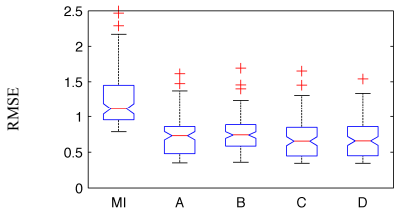

Fig 2. RMSE across 100 simulated datasets for the different analyses.

Table 1. Time to compute (s) for example dataset.

Method	MI	A	B	C	D
Angio.	0.32	0.7	212	164	498
Perfusion	0.01	0.09	78	37	120

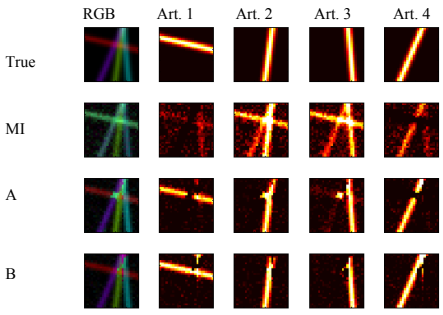

Fig1. Example of analysis results from simulated data, showing individual contributions for each artery and combined RGB image.

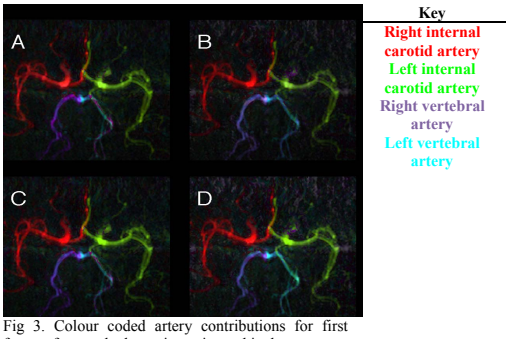

Fig 3. Colour coded artery contributions for first frame of example dynamic angiographic data.

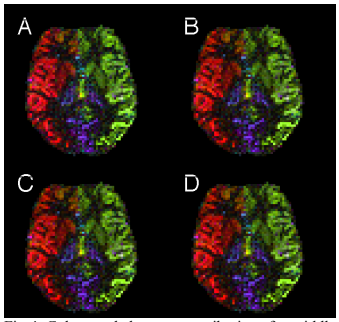

Fig 4. Colour coded artery contributions for middle slice of example perfusion data.

References:
1. Günther *et al*., MRM 56: 671-675, 2006.
2. Wong, MRM 58:1086-1091, 2007.
3. Okell *et al*., MRM 64:698-706, 2010.
4. Chappell et al., MRM, e-pub 10.1002/mrm.22524.
5. Guo & Wong, proc. ISMRM Stockholm, 2010.